Electronic Supplementary Material (ESI) for Dalton Transactions.

Synthesis of large-pore zeolites from chiral structure-directing agents with two L-prolinol units

Luis Gómez-Hortigüela, Álvaro Mayoral, Haining Liu, Laura Sierra, Laura Vaquerizo, Cristina Mompeán and Joaquín Pérez-Pariente*

Instituto de Catálisis y Petroleoquímica, ICP-CSIC. C/ Marie Curie 2, 28049. Madrid, Spain.
Corresponding Author: LGH; Email: lhortiguela@icp.csic.es

Supporting Information

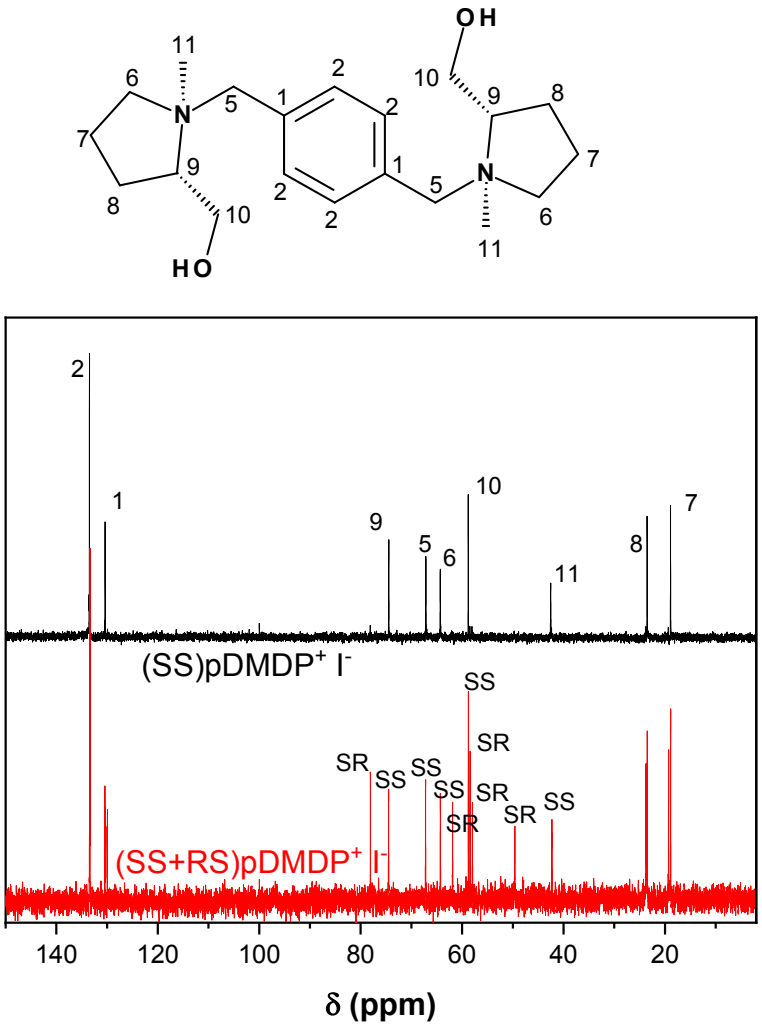

Figure S1. ^{13}C liquid NMR of pDMDPx^{+}I^{-} obtained through the two synthetic routes, by subsequent addition of para-xylene and methyl groups (top, black line) or first methyl and then para-xylene groups (bottom, red line).

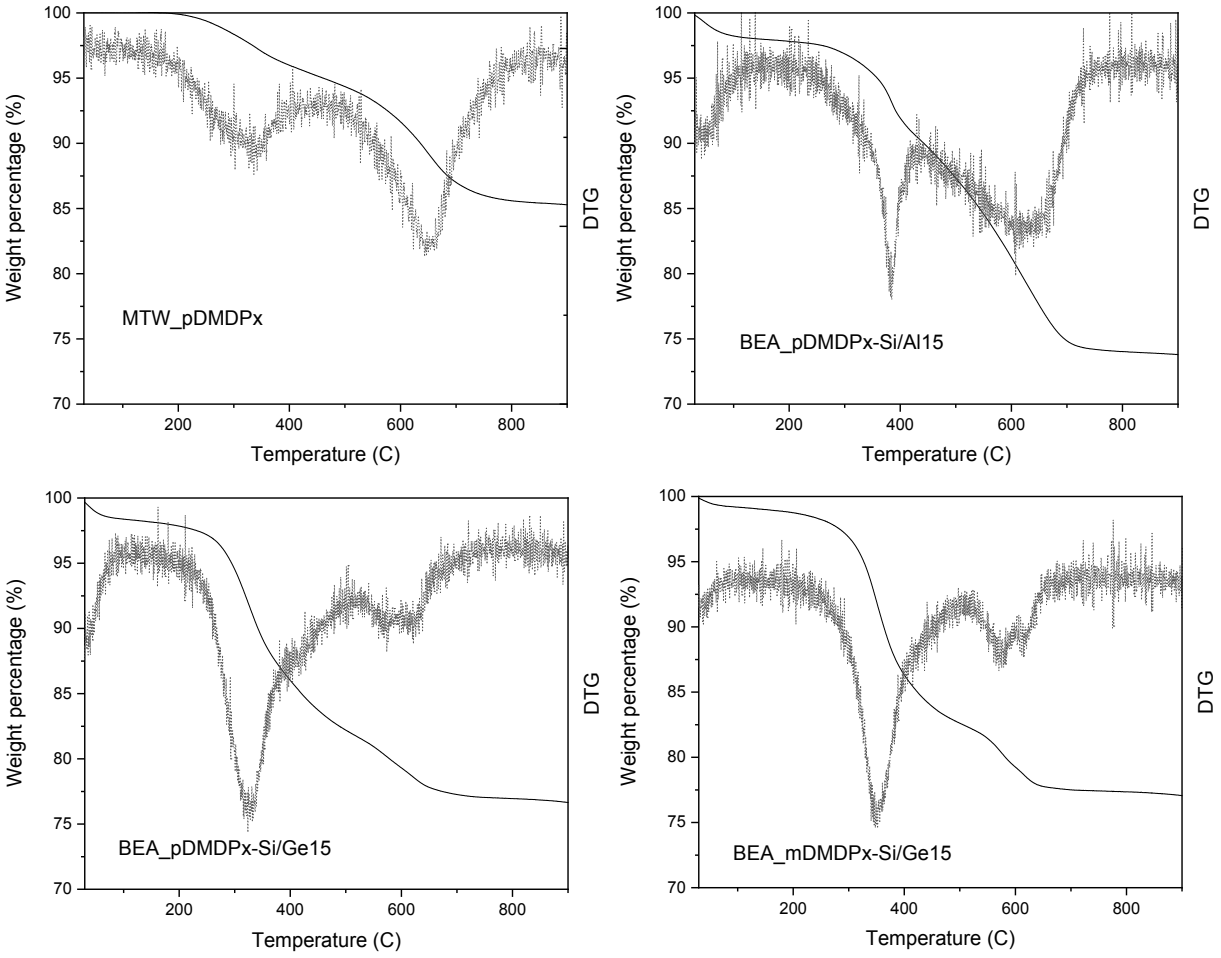

Figure S2. TGA of zeolite materials obtained with pDMDPx and mDMDPx.

Table S1. Relative energies of the different pDMDPx conformers, calculated at different levels of theory (DFT or Dreiding).

Conformer	*Orient.*	*Tors. Angle*	*R.E. (DFT)*	*R.E. (Dreid)*
pDMDPx-ss-6060	opp	60	0.8	0.8
pDMDPx-ss-300300	opp	-60	7.5	11.1
pDMDPx-ss-180180	opp	180	0.0	0.0
pDMDPx-opp-6060	ss	60	2.8	2.8
pDMDPx-opp-300300	ss	-60	2.5	7.0
pDMDPx-opp-180180	ss	180	1.0	1.8

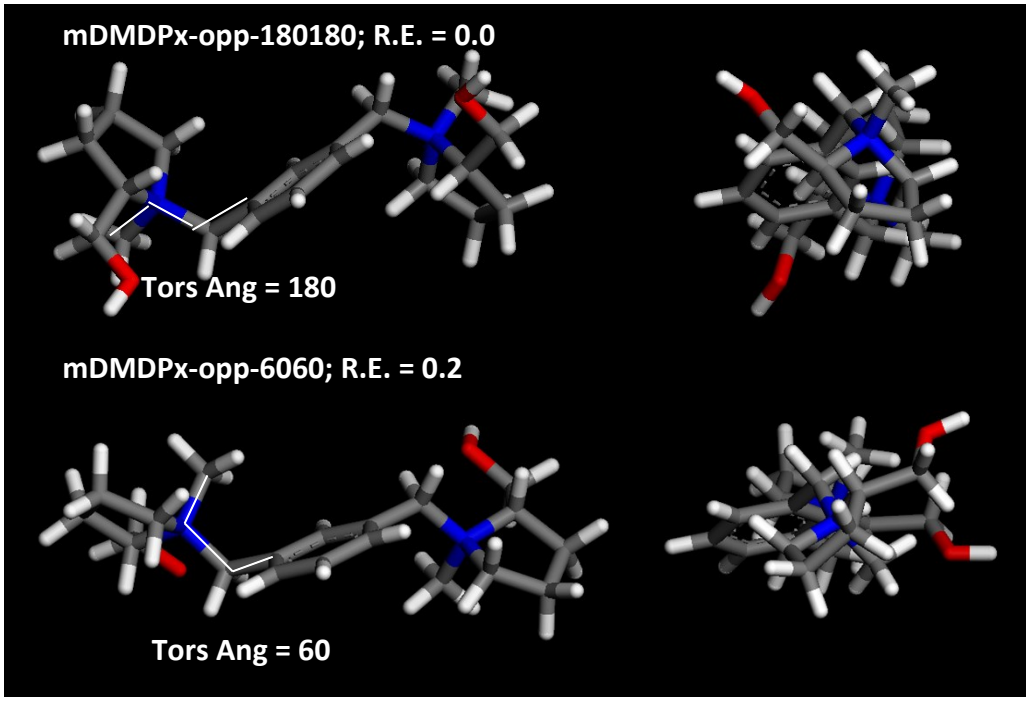

Figure S3. Molecular structure of the two most stable conformers of mDMDPx with prolinol units in opposite sides; relative energies (calculated with Dreiding method) are also reported, as well as C11-N-C5-C1 torsion angle.

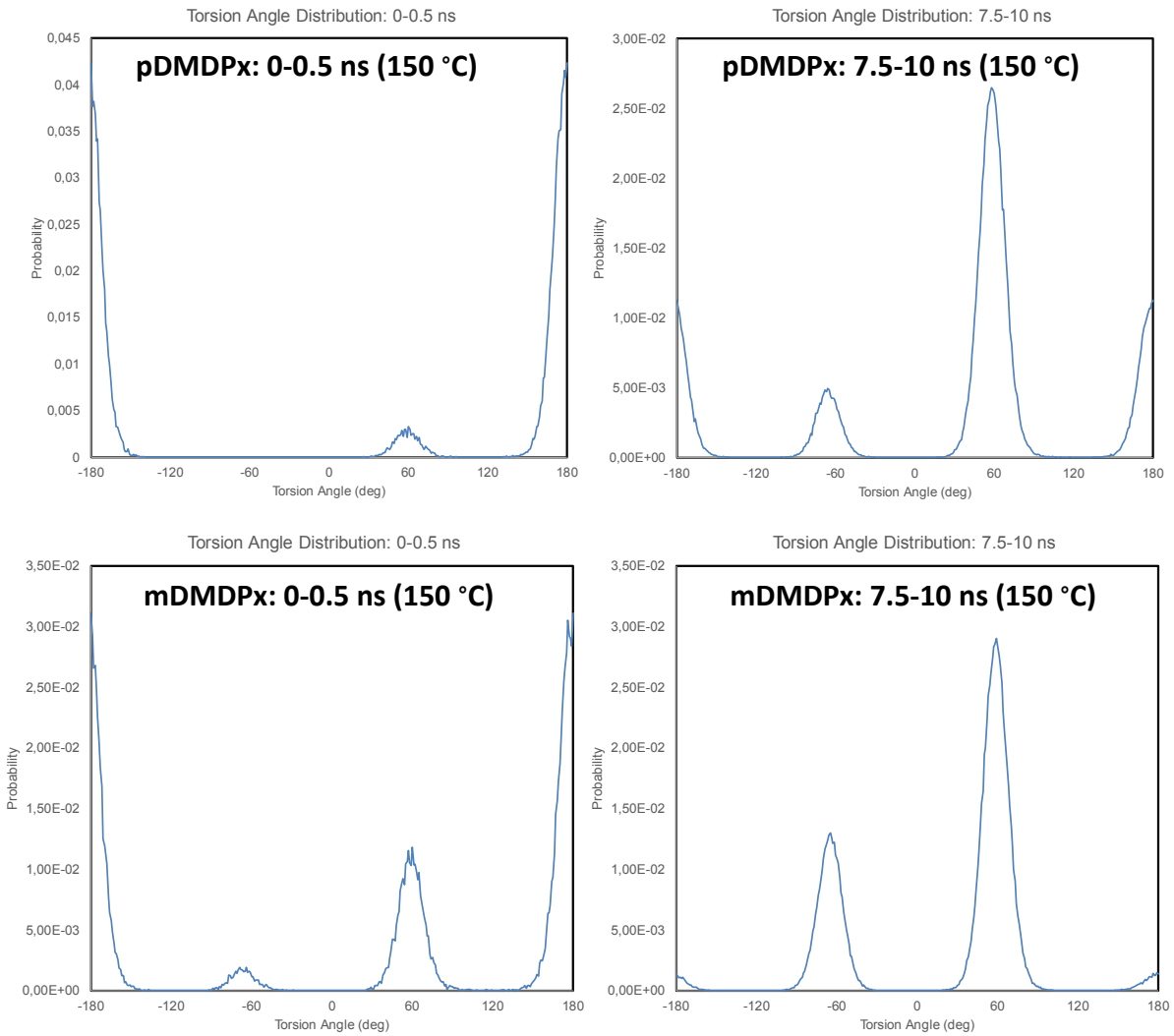

Figure S4. Distribution of conformers during MD simulations at 150 C, at the beginning (0-0.5 ns) and at the end (7.5-10 ns) time intervals for pDMDPx (top) or mDMDPx (bottom).

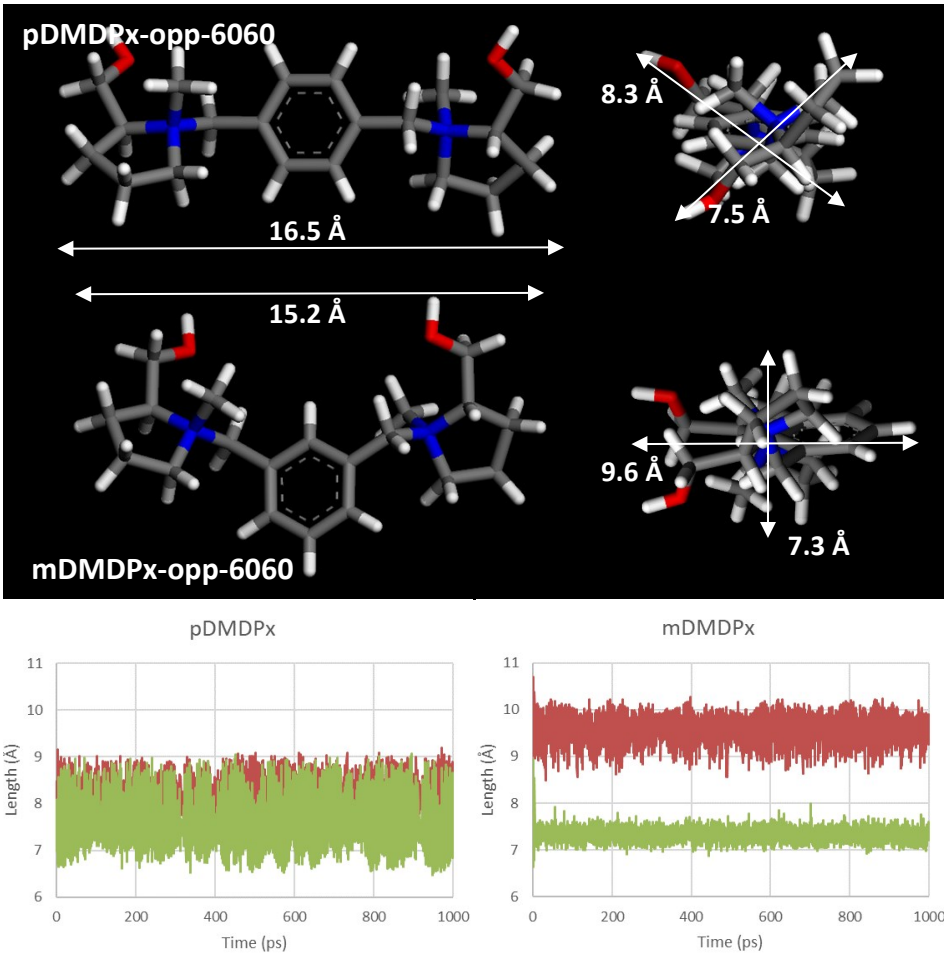

Figure S5. Geometric properties of pDMDPx and mDMDPx, characterized by their molecular shadow lengths during MD simulations in vacuo.

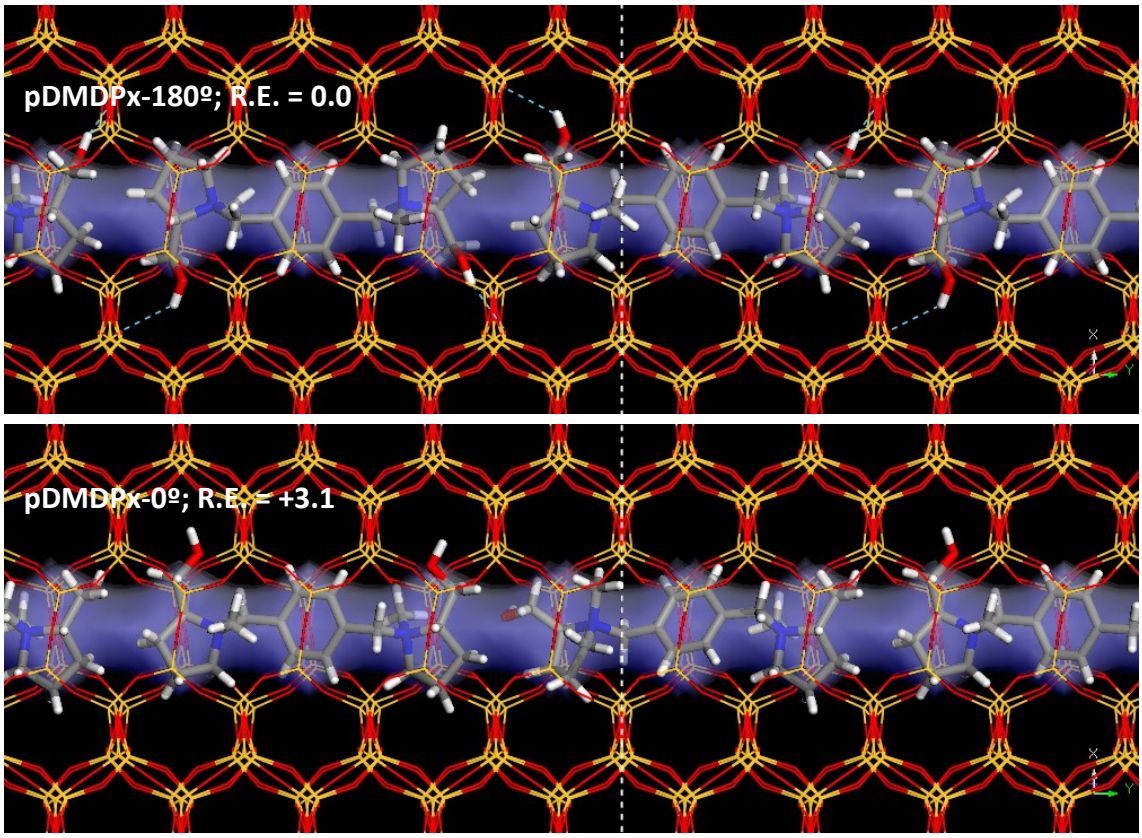

Figure S6. Packing of pDMDPx in the most stable configuration with 180º rotation (top) or no rotation (bottom) of the dications along the MTW channels.

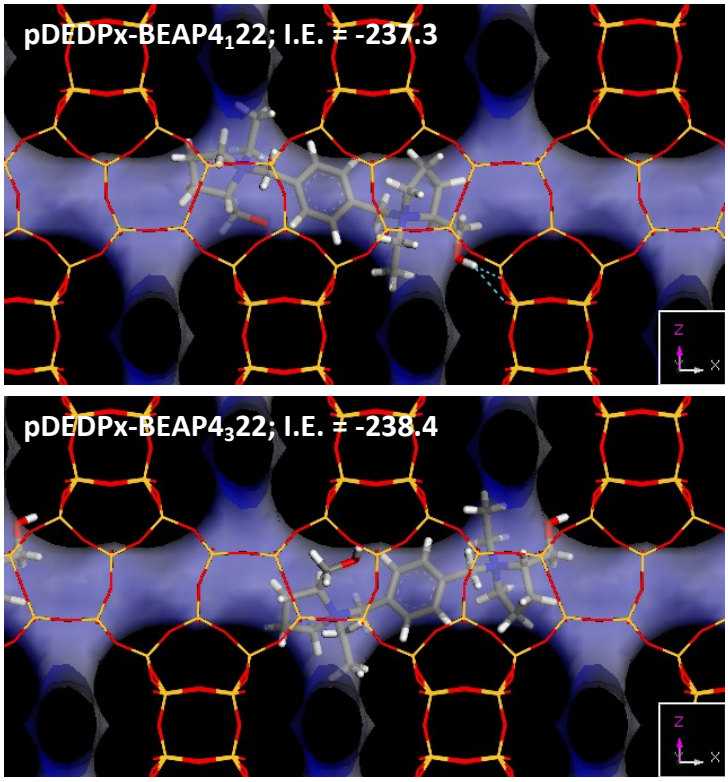

Figure S7. Most stable location of pDEDPx (1SDA per supercell) in BEA chiral polymorph A with $P4_122$ and $P4_322$ space groups, and the corresponding interaction energies.

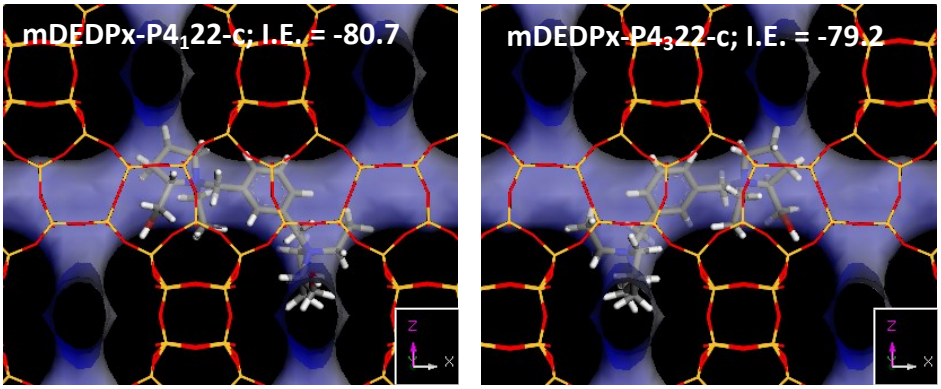

Figure S8. Most stable location of mDEDPx (1SDA per supercell) in BEA chiral polymorph A with $P4_122$ and $P4_322$ space groups, and the corresponding interaction energies.

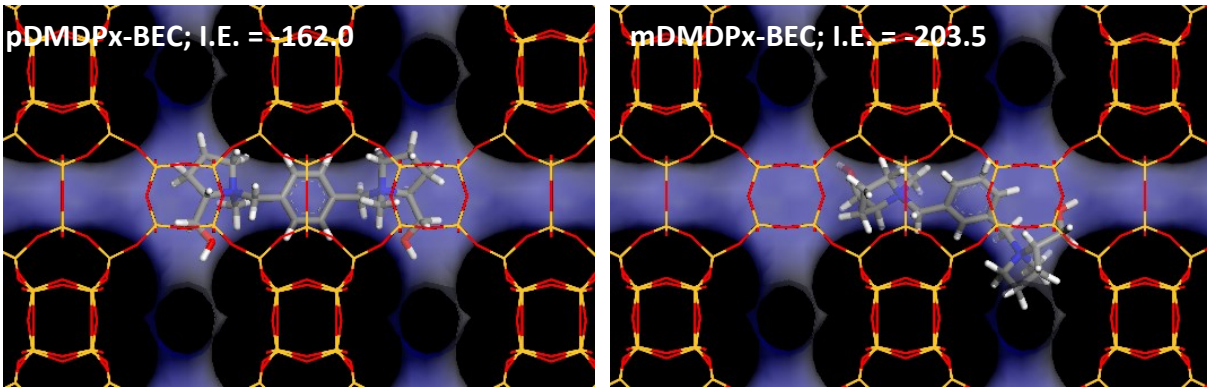

Figure S9. Most stable location (1SDA per supercell) of pDMDPx (left) and mDMDPx (right) in BEC polymorph C, and the corresponding interaction energies.